Dual wavelength laser diode excitation source for 2D photoacoustic imaging.

Thomas J. Allen and Paul C. Beard

Department of Medical Physics and Bioengineering, Malet Place Engineering Building, Gower Street, London, WC1E 6BT, UK

http://www.medphys.ucl.ac.uk/research/mle/index.htm

ABSTRACT

Photoacoustic methods can be used to make spatially resolved spectroscopic measurements of blood oxygenation when using a multiwavelength excitation source, such as an OPO system. Since these excitation sources are usually expensive and bulky, an alternative is to use laser diodes. A fibre coupled laser diode excitation system has been developed, providing two wavelengths, 850 and 905nm, each composed of 6 high peak power pulsed laser diodes. The system provided variable pulse durations (65-500ns) and repetition rates of up to 5KHz. The pulse energies delivered by the excitation system at 905nm and 850nm were measured to be $120\mu J$ and $80\mu J$ respectively for a 200ns pulse duration. To demonstrate the utility of the system, the excitation source was combined with an ultrasound detector to form a probe for *in vivo* single point measurements of superficial blood vessels. Changes in blood oxygenation and volume in the finger tip were monitored while making venous and arterial occlusions. To demonstrate the imaging capability of the excitation system, 2D photoacoustic images of a physiologically realistic phantom were obtained for a range of pulse durations using a cylindrical scanning system. The phantom was composed of cylindrical absorbing elements($\mu_a = 1mm^{-1}$) of 2.7mm diameter, immersed in a 1% intralipid solution ($\mu_s = 1mm^{-1}$). This study demonstrated the potential use of laser diodes as an excitation source for photoacoustic imaging of superficial vascular structures.

Keywords: Laser diodes, Photoacoustics, Imaging

1. INTRODUCTION

Photoacoustic imaging is a promising new technique for visualising the structure and function of soft tissues based upon the use of short laser pulses to generate broadband ultrasonic signals at depth in tissue.[1] By mapping the signals over the tissue surface, and measuring their time of flight, it is then possible to reconstruct an image of the internal tissue structure based on the absorbed optical energy distribution. The fundamental advantage of the technique is that it provides the high contrast and spectroscopic specificity of optical methods along with the high spatial resolution available to ultrasound. Since photoacoustic image contrast is, in essence, absorption based, it is particularly well suited to imaging vascular anatomy on account of the strong preferential absorption of haemoglobin. As a consequence, it has potential for the assessment soft tissue abnormalities, such as tumours, that are characterised by changes in the structure and function of the microvasculature.

In order to generate photoacoustic signals efficiently, laser pulse durations of tens to hundreds of nanoseconds are required. It is also desirable to use a wavelength in the near infrared (NIR) range (600-1200nm) where biological tissues are relatively transparent in order to obtain an adequate penetration depth. These requirements can be met, in part, by the Q-switched Nd:YAG laser operating at 1064nm. For pulse repetition frequencies (PRF) of a few tens of Hz, it can readily provide the necessary mJ pulse energies required to generate detectable photoacoustic signals in tissues. This, along with compact size, modest power requirements and relatively low cost, has led to it finding widespread use in biomedical photoacoustics. The fundamental disadvantage of the Nd:YAG is that it provides only a single fixed NIR wavelength. It cannot therefore be used for multiwavelength applications such as the spectroscopic quantification of specific tissue chromophores such as oxy and deoxy-haemoglobin.[2] Tuneable excitation sources, which can provide the necessary tuning range in the NIR, mJ

Send correspondence to T. J. Allen E-mail: tjallen@medphys.ucl.ac.uk,

Photons Plus Ultrasound: Imaging and Sensing 2007: The Eighth Conference on Biomedical Thermoacoustics, Optoacoustics, and Acousto-optics, edited by Alexander Oraevsky, Lihong V. Wang,
Proc. of SPIE Vol. 6437, 64371U, (2007) · 1605-7422/07/$18 · doi:10.1117/12.698651

pulse energies and nanosecond durations, are available in the form of Q-switched Nd:YAG pumped OPO, dye and Ti-Sapphire laser systems. Although widely used as laboratory tools, the biomedical application of these systems, particularly within a clinical environment, is limited by their high cost, large size, power and cooling requirements and practical utility (eg the need for re-alignment)

Pulsed laser diodes offer the prospect of overcoming these limitations. They are compact, relatively inexpensive and, most importantly for spectroscopic applications, readily available in a range of wavelengths in the NIR. The main disadvantage is the limited peak output power they can provide, typically <200W, in order to avoid catastrophic optical damage at the facet of the diode. This limits the pulse energies available (for nanosecond pulse durations) to a few tens of microjoules compared to the millijoule pulse energies available from Q-switched Nd:YAG based excitation systems. For this reason, laser diode based excitation systems have found limited application in photoacoustic techniques, biomedical or otherwise. Early studies tended to rely on focussing the laser output to a small spot on the surface of the target to achieve sufficient energy density for photoacoustic generation.[3,4] This approach is unsuitable for many photoacoustic applications, particularly imaging, where it is required to irradiate a relatively large tissue volume with a comparatively large area ($\sim 1cm^2$) incident beam. More recently however, 2D tomographic images of physiologically realistic targets have been obtained using a multi laser diode excitation source.[5] *In vivo* images of superficial blood vessels have also been obtained by scanning a single fiber coupled laser diode over the imaging area.[6]

Although the limited pulse energy appears at first sight to represent a fundamental limitation, there is substantial scope to mitigate this. Firstly, the PRF of a pulsed laser diode can be of the order of KHz compared to a few tens of Hz for Q-switched based excitation systems. With a suitably fast acquisition system this allows several thousand photoacoustic signals to be acquired and signal averaged in a fraction of a second with a consequent increase in signal to noise ratio (SNR). Further gains in SNR can be made by optimising the photoacoustic signal generation efficiency and the detection sensitivity: the former by selecting the laser pulse duration in relation to the geometric parameters of the target[7] and the latter by matching the bandwidth of the ultrasound receiver bandwidth to that of the generated signal. Additionally, the low cost of laser diodes and their associated drive electronics makes it economically viable to combine the output of an array of devices to increase total power output. Employing a combination of these strategies, it then becomes possible to begin closing the SNR gap between Q-switched and laser diode based excitation systems to provide a realistic alternative to current multiwavelength sources. The work presented here continues from the work previously presented in ref. 5, with the aim of demonstrating the utility of such excitation systems.

Section 2 gives an overview of a dual-wavelength laser diode excitation system that is being developed. Section 3 describes *in vivo* single point measurements of superficial blood vessels while applying arterial and venous cuff occlusions. Section 4 demonstrate the possibility of obtaining 2D photoacoustic images and a means of deconvolving for the finite pulse duration of the laser.

2. OVERVIEW OF THE EXCITATION SYSTEM.

The excitation system was composed of 12 laser diodes split equally amongst two wavelengths: 905nm and 850nm, to allow spectroscopic measurements. The peak output power provided by these devices was 175W and 100W respectively when driven with peak currents of 60A and 30A. Their duty cycle was 0.1% and 0.025% respectively, allowing each device to be driven at a repetition rate of 5KHz and 1.25KHz when using a 200ns pulse duration. Custom built drivers were used to allow the pulse duration (50ns to 500ns) and repetition rate (100Hz to 5KHz) to be varied. The output of each laser diode was coupled to an optical fiber of 1mm core diameter to guide the emitted light to the sample under investigation (see figure 1(a)). A fast data acquisition card with an on-board segmented memory architecture was used to rapidly acquire and signal average many signals in a short period of time. The on board memory of the card allowed consecutive acquisition of photoacoustic signals before downloading and signal averaging them. This avoids the rearm time of a digitising oscilloscope (∼10ms), enabling waveforms to be acquired and averaged at the true pulse repetition frequency of the laser diode. The pulse energy at 905nm and 850nm was measured at the output of the fiber bundle to be $120\mu J$ and $80\mu J$ respectively for a 200ns pulse duration. To keep the system compact the excitation source was enclosed in a standard 19 inch rack (see figure 1(b)).

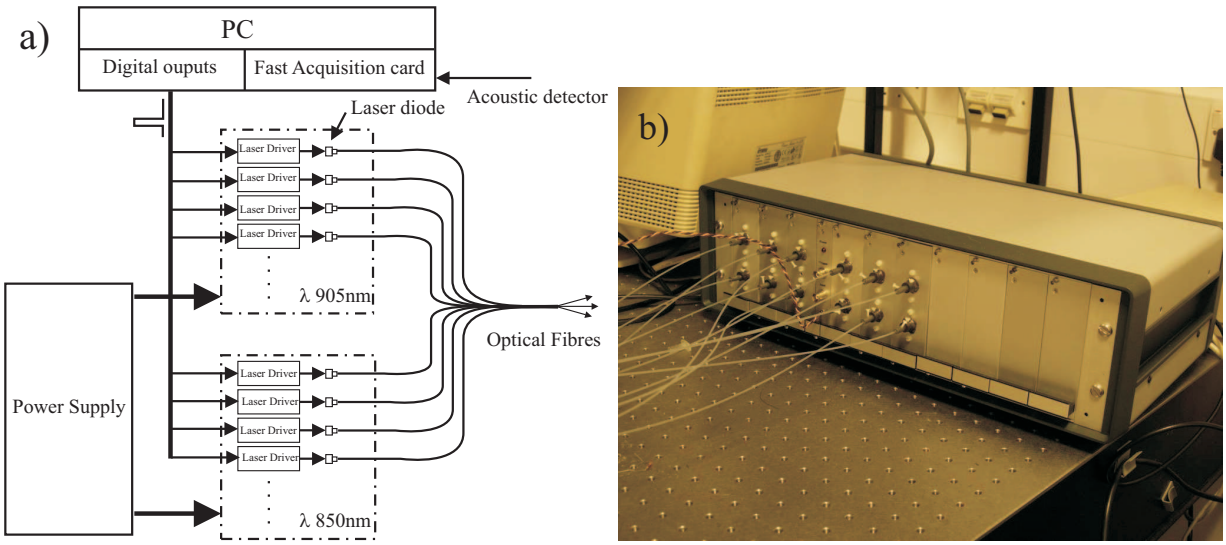

Figure 1. Laser diode excitation system (a) Schematic (b) photograph

3. IN VIVO MEASUREMENTS

To demonstrate the utility of such an excitation system for biomedical applications, *in vivo* single point measurements were made on the finger tip to monitor changes in blood oxygenation and volume while applying arterial and venous occlusions.

3.1. Methods

The laser diode excitation system was combined with a cylindrically focused ultrasound detector (PZT, 3.5 MHz) of focal length 33 mm, to form a photoacoustic probe (see figure 2(a)). The probe was composed of a water filled plastic cylinder with a stretched film of polyvinyl chloride (PVC) placed at one of the extremities and the ultrasound detector at the other. The PVC film is assumed to be optically and acoustically transparent. The optical fibers were distributed uniformly around the target area, at an angle, to illuminate the sample with a beam diameter of approximately $8mm$. The excitation system was driven at a $1KHz$ repetition rate. For a 200ns pulse duration, the output pulse energy was measured to be $120\mu J$ at $905nm$ and $80\mu J$ at 850nm. The output of the ultrasound detector was amplified ($40dB$) by a low noise amplifier before being acquired by the acquisition system, which allowed the signals to be signal averaged 1000 times in approximately 1 second.

In the first instance, a measurement was made on the thumb to demonstrate the possibility of making *in vivo* measurements. Then, the probe was placed at the tip of the middle finger and a pressure cuff was applied around the biceps. Two sets of measurements were obtained, the first during an arterial occlusion of the forearm where the pressure cuff was inflated to $200mmHg$ and the second during a venous occlusion of the forearm where the pressure cuff was inflated to $60mmHg$. Each experiment consisted of three stages; a preliminary rest stage of 30s duration, an occlusion stage of 3mins 30s and a recovery stage of 2mins. These measurements were made at both wavelengths, though only the signals obtained at 850nm are shown here, as the 905nm signals showed similar behaviour.

3.2. Results

Figure 2(b) shows the time domain signal generated in the thumb. Three bipolar signals can be seen, the first was believed to be generated by the absorption of melanin in the skin, the second which occurs at a depth of 1.2mm was thought to be generated by the absorption of blood in the dermal microvasculature and the third, which occurs at a depth of 2.025mm, was thought to be generated by the vasculature in the hypodermis (see

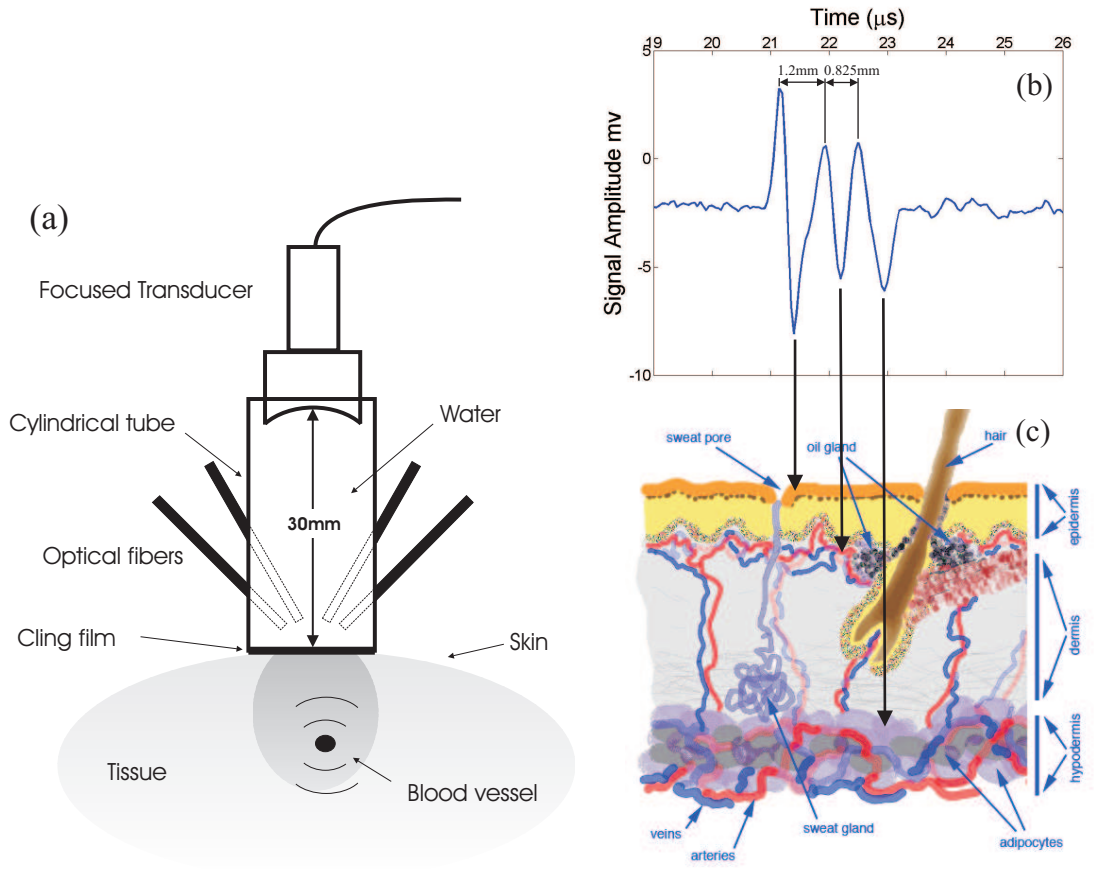

Figure 2. (a) Photoacoustic probe (b) Time domain signal generated in the thumb (c) Skin morphology[8]

figure 2(c)). The thickness of the epidermis and dermis can vary significantly depending on the region being investigated. The range of thicknesses of the epidermis and dermis are 0.03-1.4mm and 0.86-3mm respectively[9] in human adults, our measurements corresponded well with these figures.

Figure 3 shows a time domain signal generated in the tip of the middle finger. The first peak (signal 1) is though to be generated due to the absorption by melanin in the skin and the second peak (signal 2) is thought to be generated due the absorption of blood in the microvasculature lying $0.83mm$ below the surface. Figure 4(a) shows a plot of the peak to peak amplitude of signal 1 and 2 versus time, during an arterial occlusion. It can be seen that as the pressure cuff is inflated (t=30s) a drop in the peak to peak amplitude of the photoacoustic signal generated in the microvasculature occurs. This is due to a decrease in the blood oxygenation, as the oxygen is consumed and no newly oxygenated blood can flow to the finger due to the occlusion. Once the decrease starts flattening out it can be assumed that the blood is totally deoxygenated. No significant change can be noticed in the photoacoustic signal generated in the skin over the same time period. When the cuff occlusion is released (t= 240s) the photoacoustic amplitude in signal 2 increases as oxygenated blood can flow into the finger again. Figure 4(b) shows a plot of the peak to peak amplitudes of signals 1 and 2 versus time, during a venous occlusion. It can be seen that as the pressure cuff is inflated (at t=30s) the peak to peak amplitude of the photoacoustic signal generated in the microvasculature increases. This is due to the increase in blood volume in the finger tip, as blood will be able to circulate to the finger via the arteries but will not be able to leave the forearm due to the occlusion of the veins. Once the pressure is released (t=240s) the signal slowly returns to its original level.

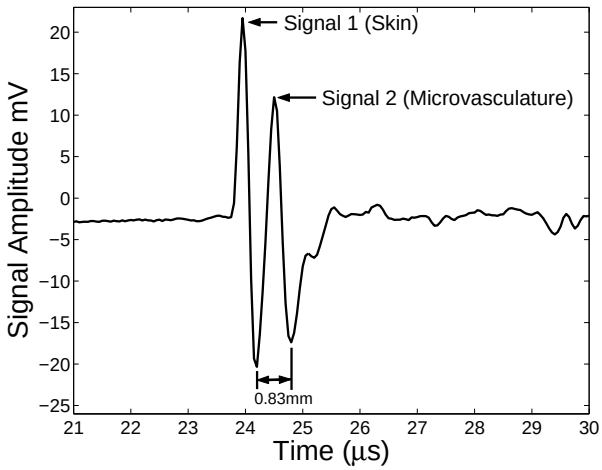

Figure 3. Photoacoustic signal measured at the tip of the finger

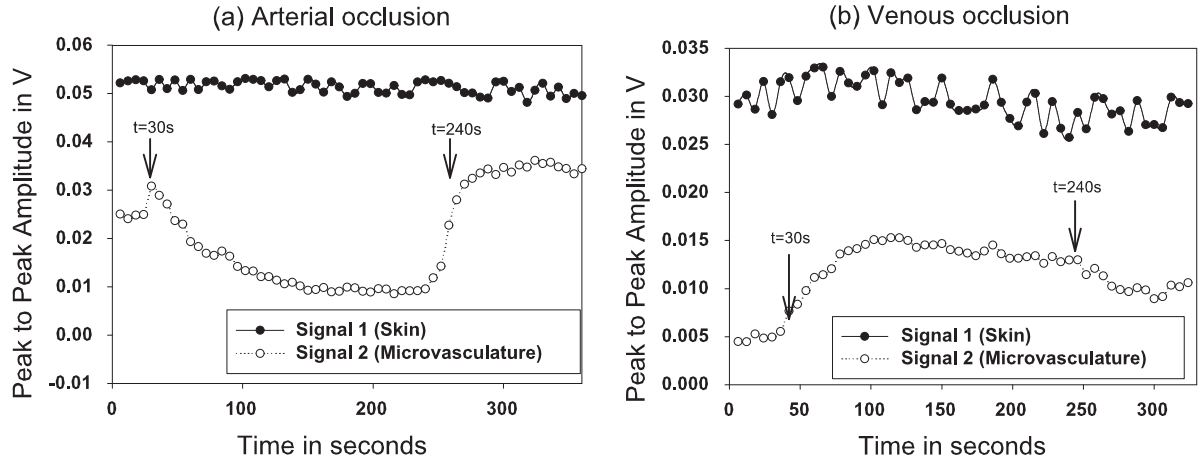

Figure 4. Measurements of the peak to peak amplitude of photoacoustic signal for (a) arterial occlusion (b) venous occlusion, the occlusions are applied and realised at t=30s and t=240s respectively.

3.3. Discussion

These results have demonstrated the possibility of making *in vivo* photoacoustic measurements of superficial blood vessels using a laser diode excitation system. The detected signals have provided information about the spatial distribution (1D) of the absorbed optical energy in tissue, the first and second bipolar photoacoustic signals are thought to correspond to the optical energy absorbed by the skin layer and the microvasculature respectively. At the time, it was not possible to spectroscopicaly analyse the data to determine blood oxygen saturation. This was because the detected signal could not be normalised for each wavelength due to errors in measuring the incident fluence distribution over the tissue. In addition, to obtain accurate spectroscopic measurements of blood oxygenation at least one additional wavelength would be required. However, the ability to monitor changes in the blood oxygenation and volume was demonstrated.

4. 2D PHOTOACOUSTIC IMAGING

To further demonstrate the utility of the excitation system it was combined with a cylindrical scanner, to provide 2D photoacoustic images of a tissue mimicking phantom.

4.1. Methods

The cylindrical scanner was composed of a stepper motor under PC control which could rotate a cylindrically focused PZT (3.5MHz) detector of focal length 33 mm, around the sample under investigation (see figure 5(a)). The detector was scanned through 306^o in 3.6^o steps, a full scan of 360^o could not be achieved as the scanning path was partially obstructed by the fiber bundle used to deliver the light. The scanning radius was 25mm. For these experiments only four 905nm high peak power pulsed laser diodes were used, providing total pulse energies of $E = 24\mu J$ and $E = 184\mu J$ for laser pulse durations of $t_p = 65ns$ and $t_p = 500ns$ respectively. The detected photoacoustic signal was amplified (40dB) and signal averaged before being downloaded to a PC at each angular increment of the scan. The signals were then used in a modified back projection algorithm[10] to reconstruct a 2D image. The phantom was composed of three cylindrical absorbing elements (diameter 2.7mm and thickness 1mm). These elements were formed out of gelatine, mixed with a dye whose absorption coefficient is similar to blood (μ_a=1mm^{-1}). Figure 5(b) shows these three elements as they were in the phantom, before a gel mixture containing 1% intralipid (μ_s=1mm^{-1}) mimicking the scattering properties of tissue was poured on top, immersing the absorbing elements to a depth of $4mm$.

4.2. Results

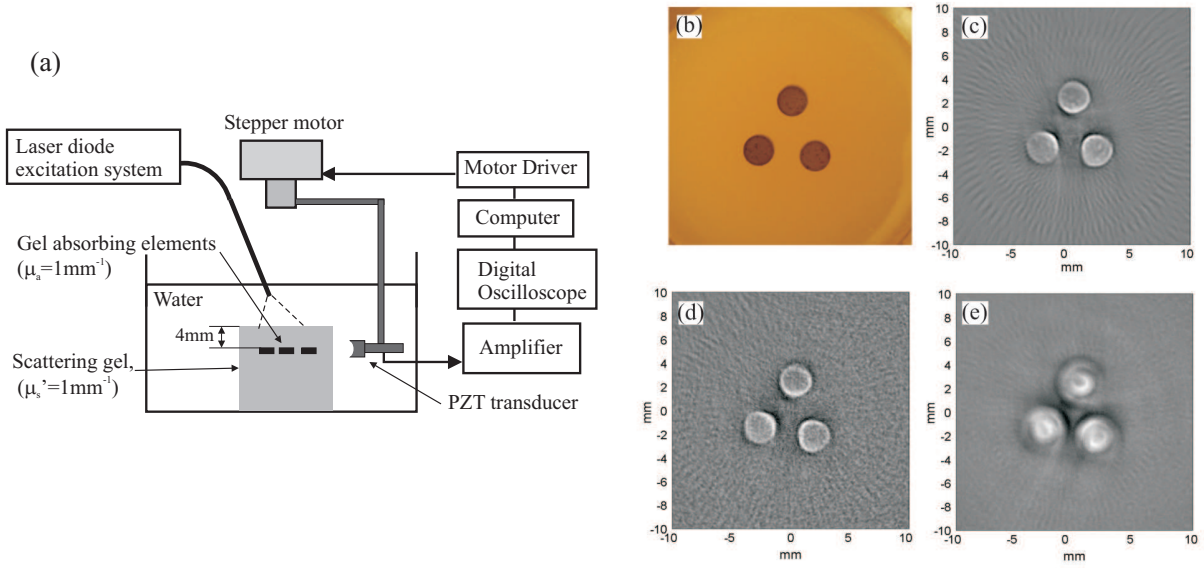

Figure 5. (a) Cylindrical scanning system (b) Photograph of the phantom before adding the top layer of the scattering medium (c) Reconstructed photoacoustic image obtained using the Q-switched Nd:YAG laser, t_p=7ns, (d) and (e) images obtained using the laser diode system for using t_p=65ns and t_p=500ns

An image was first obtained using a Q-switched Nd:YAG laser operating at 1064nm for comparison purposes. The pulse energy was 10mJ, t_p=7ns and the detected signals averaged over 20 shots. The reconstructed image is shown in Figure 5(c) and correlates well with the photograph of the phantom (figure 5(b)). Figures 5(d) and 5(e) show the images obtained using the laser diode excitation system for t_p=65ns and t_p=500ns respectively and signal averaging over 5000 pulses.

4.3. Discussion

These images illustrate a compromise between SNR and spatial resolution. For the longer pulse duration, the SNR is approximately a factor of 5 higher but the spatial fidelity of the reconstructed image is relatively poor with the absorbing cylinders barely distinguishable from each other. For the shorter pulse duration the resolution is much improved and, although the SNR is significantly reduced, the objects are clearly identifiable and

compare well to the image in (c) obtained with the Nd:YAG laser. Also increasing the pulse duration downshifts the acoustic frequency spectrum of the signals and therefore limits the spatial resolution of the reconstructed image. It should be possible to retrieve high resolution images while keeping the improved SNR by deconvolving the signal with the temporal shape of the pulse duration. This is due to the fact that the delivered pulse energy will increase proportionally with pulse duration, therefore the absolute amplitudes of the high frequency components for the longer pulse duration may be comparable or exceed those generated by a shorter pulse. The retention of the higher frequency components (assuming they are above the noise floor) offers the prospect of using deconvolution to improve spatial resolution of the images.

The photoacoustic signal $g(t)$ generated by a finite pulse duration corresponds to the temporal shape of the pulse duration $K(t)$ convolved with the photoacoustic signal when generated by an impulse $f_0(t)$,

$$g(t) = \int K(t-t')f_0(t')dt' \Longrightarrow g(w) = K(w)f_0(w) \tag{1}$$

With exact knowledge of both $K(w)$ and $g(w)$, it is possible to deconvolve the signals to obtain an accurate value of $f_0(w)$ using the following equation

$$f_0(w) = \frac{g(w)}{K(w)} \tag{2}$$

However, for practical measurements, noise will be present and the bandwidth limited by the instrumentation. Therefore equation 2 can be rewritten to include noise.

$$f(w) = \frac{g_n(w)}{K_n(w)} = \frac{g(w) + n_g(w)}{K(w) + n_K(w)} \tag{3}$$

where $n_K(w)$ and $n_g(w)$ are the noise contribution to the signals $g_n(w)$ and $K_n(w)$ respectively. This can cause significant problem when deconvolving. First if $K(w) = 0$, $g(w)$ is also expected to be zero, however due to noise being present, $f(w) = \frac{n_g(w)}{n_K(w)}$ and therefore $f(w)$ will be directly dependent on the noise values. Secondly if $K(w) + n_K(w) = 0$ there will be a division by zero and $f(w)$ will be infinite. Finally, in practical situations, the signal will be bandlimited, thus as w tends to infinity $K(w)$ becomes relatively small and may be zero. In this region the deconvolution errors in the computed $f(w)$ will be large and $f(w)$ will be an erroneous estimated of $f_0(w)$.

A first approach is to design a restoring filter function $C(w)$ using a constrained least square solution.[11–13]

$$f_e(w) = g_n(w)C(w) \tag{4}$$

$$C(w) = \frac{K_n^*(w)}{|K_n(w)|^2 + \mu} \tag{5}$$

where $f_e(w)$ is an estimate of $f_0(w)$, K_n^* is the complex conjugate of K_n and μ is a parameter that controls the balance between the degree of noise reduction and the errors introduced by the filter. This can be rewriten to give

$$f_e(t) = \frac{1}{2\pi}\int \frac{K_n^*(w)}{|K_n(w)|^2 + \mu} g_n(w)e^{iwt}dw \tag{6}$$

Figure 6 shows a reconstructed 2D photoacoustic image using the data provided by the 500ns duration pulse after deconvolving each acquired photoacoustic signal with the temporal shape of the finite pulse duration using

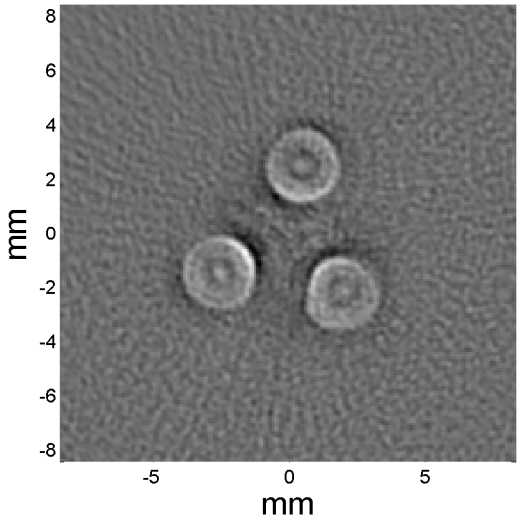

Figure 6. Image obtained after deconvolving the data used to reconstruct the image in figure 5(e) with the temporal shape of a 500ns pulse duration.

equation 6. The regularisation parameter μ was set to a constant values, which was chosen to produce the best reconstructed image. It can be seen that the spatial resolution of the images has been retrieved and correlates well with the images obtained using the short pulse duration (figure 5(d)) or the Q-switched laser (figure 5(c)). This was a first attempt at deconvolving for the laser pulse duration. Improved results may be achieved by optimising the regularisation parameter μ for each signal instead of using a constant value for all, using different constraints or trying to deconvolve the reconstructed image instead of each individual photoacoustic signal.

5. CONCLUSION

This study has shown that a laser diode excitation system can generate detectable signals in superficial blood vessels with sufficient SNR to monitor changes in blood oxygenation and volume. It was also demonstrated that such a system could be used to obtain 2D images of a physiologically realistic phantom. Future work will focus on adding extra wavelengths to enable spectroscopic measurements of blood SO2 to be made. This excitation system could be used in applications such as the study of oxygen heterogeneity in tumours and other tissue abnormalities characterised by changes in the oxygenation or perfusion of the tissue.

ACKNOWLEDGMENTS

This work has been supported by the Engineering and Physical Sciences Research Council, UK

REFERENCES

1. M. Xu and L. Wang, "Photoacoustic imaging in biomedicine," *Rev. Sci. Inst.* **77**, p. 041101, 2006.
2. J. G. Laufer, D. T. Delpy, C. E. Elwell, and P. C. Beard, "Quantitative spatially resolved measurement of tissue chromophore concentrations using photoacoustic spectroscopy: application to the measurement of blood oxygenation and haemoglobin concentration," *Physics in Medicine and Biology* **52**, pp. 141–168, 2007.
3. A. Duncan, J. Hannigan, S. S. Freeborn, P. W. H. Rae, B. McIver, F. Greig, E. M. Johnston, D. T. Binnie, and H. A. MacKenzie, "A portable non-invasive blood glucose monitor," *8th int. conf. on Solid-State Sensors and Actuators, and Eurosensors IX* **2**, pp. 455–458, 1995.

4. Z. Zhao, "Pulsed photoacoustic techniques and glucose determination in human blood and tissue," *Phd Thesis, University of OULU* , 2002.
5. T. J. Allen and P. C. Beard, "Pulsed NIR laser diode excitation system for biomedical photoacoustic imaging," *Optics Letter* **31((23)**, pp. 3462–3464, 2006.
6. R. G. M. Kolkman, W. Steenbergen, and T. Leeuwen, "In vivo photoacoustic imaging of blood vessels with a pulsed laser diode," *Lasers in Medical Science* **21**, pp. 134–139, 2006.
7. T. J. Allen, B. T. Cox, and P. C. Beard, "Generating photoacoustic signals using high-peak power pulsed laser diodes," *Proc. SPIE* **5696**, pp. 233–242, 2005.
8. "https://www.brooklyn.cuny.edu/bc/ahp/lad/c4d/c4d_skin.html/tables."
9. D. Ghodgaonkar, O. P. Gandhi, and M. F. Iskander, "Complex permittivity of human skin in vivo in the frequency band 26.5-60 Ghz," *IEEE Antennas and Propagation Society International Symposium* **2**, pp. 1100–1103, 2000.
10. M. Xu and L. V. Wang, "Time-domain reconstruction algorithms and numerical simulations for thermoacoustic tomography in various geometries," *IEEE Transactions on Biomedical Engineering* **50**(9), pp. 1086–1098, 2003.
11. B. Parruck and S. M. Riad, "An optimizationcriterion for iterative deconvolution," *IEEE Transactions on instrumentation and measurement* **IM-32**, pp. 137–140, 1983.
12. A. Bennia and S. M. Riad, "An optimization technique for iterative frequency-domain deconvolution," *IEEE Transactions on instrumentation and measurement* **39**, pp. 358–362, 1990.
13. M. Bertero and P. Boccacci, *Introduction to Inverse Problems in Imaging*, Institute of Physics Publishing, Bristol and Philadelphia, 2002.